Available online at www.sciencedirect.com
SCIENCE DIRECT
Surface Science 600 (2006) 651–656
SURFACE SCIENCE
www.elsevier.com/locate/susc

# Nucleation and growth of calcium–phosphate on Ca-implanted titanium surface

Youtao Xie [a,b], Xuanyong Liu [a,b], Paul K. Chu [b,*], Chuanxian Ding [a]

[a] Shanghai Institute of Ceramics, Chinese Academy of Science, 1295 Dingxi Road, Shanghai 200050, China
[b] Department of Physics and Materials Science, City University of Hong Kong, Tat Chee Avenue, Kowloon, Hong Kong

Received 3 March 2005; accepted for publication 21 November 2005
Available online 19 December 2005

**Abstract**

Calcium phosphate formation on Ca-implanted titanium surfaces is studied. Experimental results show that octacalcium phosphate (OCP) is the more energetically favorable phase to precipitate on the positively charged Ca-implanted titanium surfaces compared to hydroxylapatite (HA), especially with the existence of a large amount of $CO_3^{2-}$ ions. A solution-based cluster theory is employed to explain the process of the formation of calcium phosphate on the Ca-implanted titanium surfaces. Thermodynamic and kinetic calculations show that OCP is the kinetically favored phase to precipitate in the SBF solution than HA. The nucleation rate is much higher than that of HA, but HA is more stable thermodynamically.


*Keywords:* Nucleation; Calcium phosphate; Calcium; Implantation; Titanium

## 1. Introduction

Biologically active calcium (Ca) ions have been implanted into titanium surface to enhance the bioactivity and biocompatibility [1–6]. Liu et al. [1] and Hanawa et al. [2] have found that Ca ion implantation improves the ability of titanium to induce the formation of calcium phosphate (Ca–P) minerals on the surface. The results of Pham et al. [3] show a higher ability to nucleate hydroxyapatite (HA) on the implanted surface compared to the unmodified titanium surface. High dose of Ca implantation ($1 \times 10^{17}$ ions $cm^{-2}$) into titanium alloy has also been shown to significantly enhance MG-63 cell adhesion and spreading [4]. In vivo experiments show that early bone formation on Ca-implanted titanium surface is superior to that on unimplanted samples [5]. In our previous work [7], Ca ions were implanted into titanium by plasma ion immersion implantation (PIII) and Ca–P was found to nucleate on the Ca-implanted surface after immersion in a simulated body fluid (SBF) solution for 14 days. The improvement in the biocompatibility and bioactivity of the Ca-implanted titanium was attributed to the modified surface mainly consisting of calcium oxide and calcium titanate [8,9]. The surface layer was found to be composed of calcium hydroxide and calcium carbonate after calcium PIII [7,10]. The large amount of Ca ions dissolved from this surface layer induces precipitation of calcium phosphate due to supersaturation in the bioliquid near the materials.

Previous studies on Ca–P growth in in vitro models suggest that Ca–P precipitation is initiated by heterogeneous nucleation. Three kinds of driving forces are thought to take place during the nucleation process in the solid–aqueous solution systems: electrostatic interaction, London Van der Waals interaction, and hydration interaction. Among them, the electrostatic interaction is regarded as the main factor in inducing nucleation of Ca–P. Yamashita et al. [11] demonstrated that heterogeneous nucleation of Ca–P could only take place on negatively charged surface. In our previous work [12], it was found that HA could only crystallize and grow on a negatively charged wollastonite

* Corresponding author. Tel.: +852 2788 7724; fax: +852 2788 9549.
*E-mail address:* paul.chu@cityu.edu.hk (P.K. Chu).

0039-6028/$ - see front matter 
doi:10.1016/j.susc.2005.11.016

coating surface. Chloride ions but not phosphate ions were found to concentrate on the positively charged surface resulting from the lower charge density of the phosphate ions [13]. On the Ca-implanted titanium surface, due to the dissociation of hydroxyl radicals, the surface is more positively charged as measured by Hanawa [14]. However, the mechanism of how a Ca-implanted titanium modified layer induces the precipitation of the Ca–P is not well understood.

In the work reported here, we investigate the precipitation mechanism of Ca–P on Ca-implanted titanium. Thermodynamic and kinetic analyses are conducted and a solution-based nucleation mechanism is used to explain the precipitation of Ca–P on the Ca-implanted titanium surface.

## 2. Experimental procedures

Commercial polycrystalline titanium discs 10 mm in diameter and 1 mm thick were plasma implanted with calcium and the experimental setup and details have been described elsewhere [7]. The Ti discs were polished to an average roughness of less than 20 nm. Before Ca implantation, the Ti surfaces were cleaned by sputtering with argon for 5 min. The Ca-implanted titanium discs were ultrasonically washed in acetone and deionized water before submerging in SBF solutions that have ionic concentrations nearly equal to those in human body blood plasma [15]. The system pH value was buffered at 7.4 with trimethanol aminomethane–HCl. The samples were immersed in a 30 ml SBF solution for 1, 4, 7, 10, and 14 days, respectively at 36.5 °C without stirring. The changes in the concentrations of calcium and phosphorus in the SBF solutions after immersion were measured by inductively coupled plasma atomic emission spectroscopy (ICP-AES).

Scanning electron microscopy (SEM) was performed to investigate the morphologies of the precipitated Ca–P layer after incubation in SBF. The structure and phase composition of the Ca–P layer were analyzed by thin film X-ray diffraction (TFXRD) and X-ray photoelectron spectroscopy (XPS).

## 3. Theory of nucleation and growth

### 3.1. Thermodynamics of nucleation and growth

The thermodynamic driving forces for Ca–P precipitation can be calculated based on the classical equation of free energy changes in a supersaturated solution [16]:

$$\Delta G = -\frac{RT}{n}\ln(S) = -\frac{RT}{n}\ln(A_{\mathrm{p}}/K_{\mathrm{sp}}), \tag{1}$$

where $\Delta G$ is the Gibbs energy per mole of the ionic unit composed of Ca–P in the solution, $R$ is the gas constant ($8.314\ \mathrm{J\,K^{-1}\,mol^{-1}}$), $T$ is the absolute temperature, $n$ is the number of the ion unit in a Ca–P molecule, and $S$ is the supersaturation that is defined by the ratio of the activity product of the ion unit composing the precipitates ($A_{\mathrm{p}}$) to the corresponding solubility product ($K_{\mathrm{sp}}$). The negative logarithms of the ionic activity products in the SBF solution are $93.5 \pm 0.2$ for HA and $45.1 \pm 0.1$ for OCP [17]. The negative logarithms of the solubility products of HA and OCP are 115.0–118.7 [18,19] and 46.9–49.6 [20], respectively.

### 3.2. Kinetics of nucleation and growth

In the kinetic analysis, the nucleation rate ($J$) is an important factor effecting the precipitation of Ca–P, and it can be estimated based on the classical model of heterogeneous nucleation [21]:

$$J = K\exp\left(-\frac{\Delta G}{kT}\right) = K\exp\left(-\frac{16\pi v^2\gamma^3 f(\theta)}{3k^3T^3(\ln S)^2}\right). \tag{2}$$

In Eq. (2), $k$ is the Boltzmann constant and $T$ is the absolute temperature. It can be seen from the equation that the nucleation rate is proportional to the kinetic factor $K$ and exponentially affected by the activation energy of nucleation ($\Delta G$), which is related to the interfacial tension ($\gamma$) between the Ca–P phase and the solution, the supersaturation ($S$), as well as the contact angle function $f(\theta)$. The molecular volumes ($v$) of HA and OCP are 263.24 and 310.59 Å$^3$, respectively [22,23].

The kinetic factor $K$ is proportional to the probability ($P$) that the appropriate ion unit of Ca–P needed to compose a nucleus in the solution, i.e., $K = K'P$. The $P$ values can be calculated by the method of Boistelle and Lopez-Valero [22] as follows:

$$P = \frac{9![\mathrm{Ca}^{2+}]^5[\mathrm{PO}_4^{3-}]^3[\mathrm{OH}^-]}{5!3!([\mathrm{Ca}^{2+}]+[\mathrm{PO}_4^{3-}]+[\mathrm{OH}^-])^9} \quad \text{for HA} \tag{3}$$

$$P = \frac{7![\mathrm{Ca}^{2+}]^4[\mathrm{HPO}_4^{2-}][\mathrm{PO}_4^{3-}]^2}{4!2!([\mathrm{Ca}^{2+}]+[\mathrm{PO}_4^{3-}]+[\mathrm{HPO}_4^{2-}])^7} \quad \text{for OCP} \tag{4}$$

$K'$ is $13.64 \times 10^{-24}\ \mathrm{cm^{-3}\,s^{-1}}$ based on the experimental studies of Boistelle and Lopez-Valero [22].

## 4. Results and discussion

Fig. 1 shows the survey X-ray photoelectron spectroscopy (XPS) spectra acquired from the titanium samples before and after Ca-implantation. Titanium is easily oxidized to $TiO_2$ upon exposure to air, and the thickness of the $TiO_2$ is about 4 nm [24]. In the XPS measurements, 10 nm was pre-sputtered to clean surface contaminants and so only metal Ti peaks can be observed in the spectrum as shown in Fig. 1a. In contrast, after Ca-implantation, C, Ca, O can be found in the surface layer. The calcium oxide on the titanium surface reacts with ambient water to form calcium hydroxide (H cannot be detected by XPS) and then, calcium hydroxide further reacts with carbon dioxide in air to form calcium carbonate. These two phases were also found in our previous XRD and FTIR analyses [7].

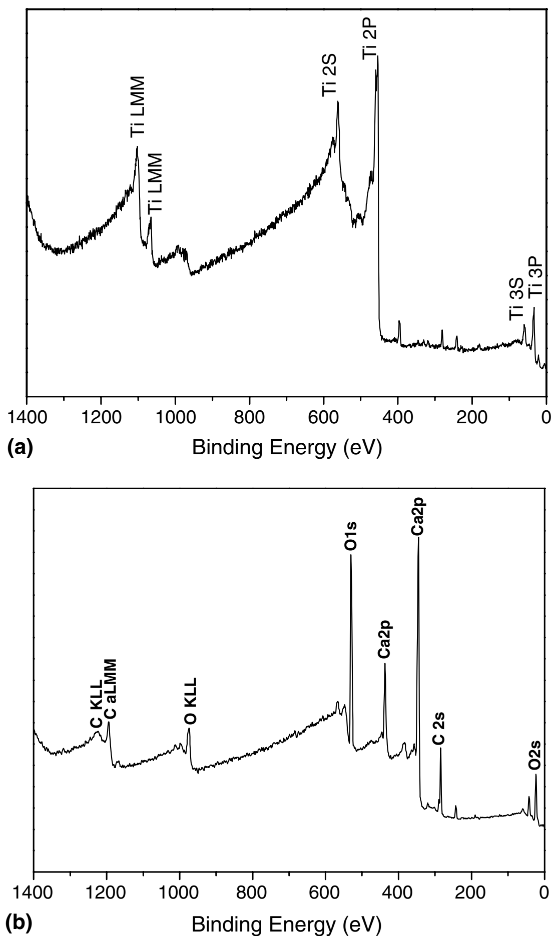


Fig. 1. XPS results acquired from titanium before (a) and after Ca-implanted (b).

Fig. 2 displays the morphologies of the Ca-implanted titanium surfaces after incubation in SBF solution for different time durations. A Ca–P film can be found on the surface after 7 days incubation in SBF. After a longer incubation time, some globular particles appear on the film. The phase of the film is measured by TFXRD and the results are shown in Fig. 3. The X-ray diffraction pattern shows typical peaks of OCP as well as titanium after incubation in SBF for 7 days. The peak at 4.7° is the typical (100) reflection of OCP although we cannot differentiate the peaks of the OCP from HA in the $2\theta$ range of 20–40°. The weak peaks at 9.4° and 9.7° confirm the existence of OCP corresponding to the (200) and (010) reflection of OCP. The peaks at 4.7°, 9.4°, and 9.7° disappear and those at near 26° and 32° become more intense after 14 days of incubation. It can be deduced that the first precipitation phase on the Ca-implanted titanium surface is OCP. Subsequently, after precipitation of OCP in the first stage, supersaturation in the solution decreases and the interfacial chemistry changes. The thermodynamically more stable phase of HA precipitates in the second stage or the original precipitated OCP transforms to HA after incubation in SBF for a relatively long time. After 14 days of immersion

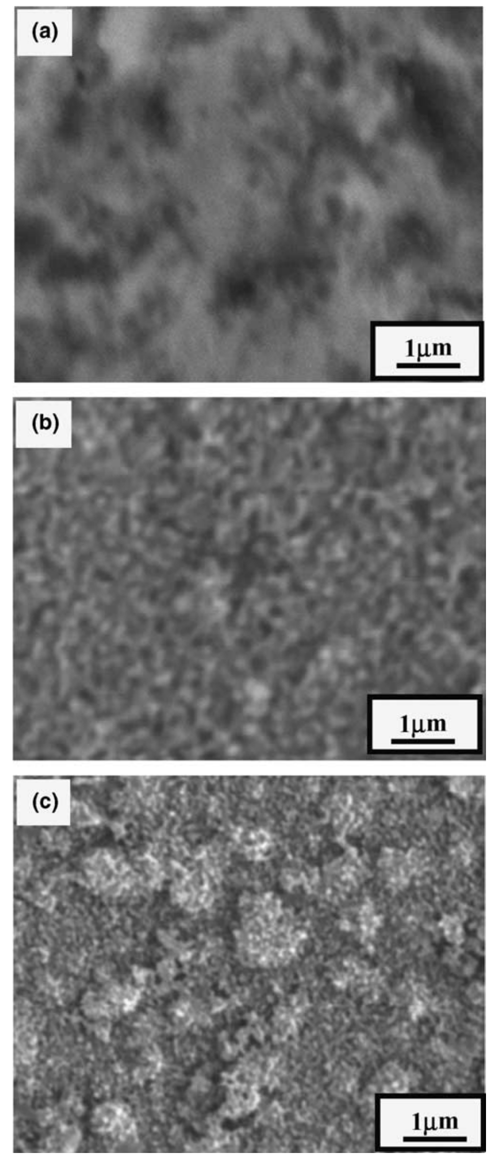


Fig. 2. SEM views of the Ca-implanted titanium: (a) as-implanted, (b) after incubation in SBF for 7 days, (c) after incubation in SBF for 14 days.

in SBF, the thickness of the deposited Ca–P layer is about several micrometers.

With precipitation of the Ca–P minerals, the calcium and phosphorus elemental concentrations in the SBF solution decreases with immersion time. Changes in the SBF solutions as monitored by ICP are illustrated in Fig. 4. The calcium concentration (right axis) shows a slight increase in the first day and then decreases in the remaining immersion time while the phosphorus concentration (left axis) decreases throughout the immersion time. It is also noticed that the consumed ratio of Ca/P in the SBF solution is much lower than that of OCP or HA. It indicates that some of the calcium dissolves from the Ca-implanted titanium discs and then nucleates with phosphorus in the solution.

Many factors affect the nucleation and growth of Ca–P in the SBF solution. Three types of driving forces are

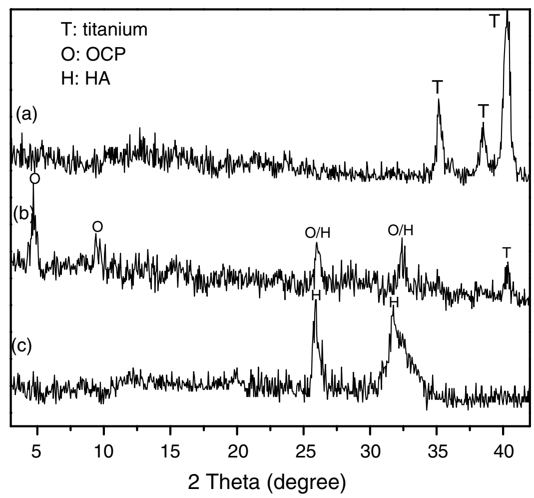


Fig. 3. TFXRD patterns of: (a) non-implanted titanium, (b) Ca-implanted titanium incubated in SBF for 7 days, and (c) Ca-implanted titanium incubated in SBF for 14 days.

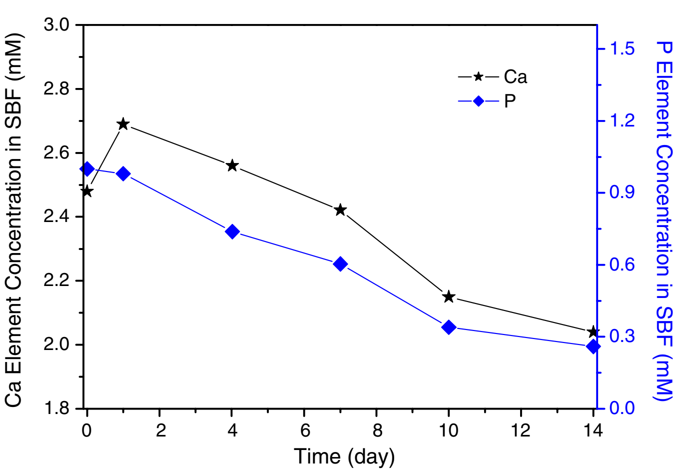


Fig. 4. Elemental concentration changes in the SBF solutions: (★) calcium, (♦) phosphorus.

believed to be involved during the nucleation process in the solid–aqueous solution system: electrostatic interaction, London Van der Waals interaction, and hydration interaction. Among them, the electrostatic interaction is believed to be the most important factor in inducing Ca–P nucleation. Yamashita et al. [11] reported that the Ca–P mineral apatite grew rapidly on the negative-pole but not on the positive-pole surface. Our previous work on wollastonite coatings also illustrates that apatite can only precipitate on a negatively charged surface. The negatively charged surface attracts calcium ions thereby increasing the local nucleation rate of apatite from the solution. One may also expect the negative surface to deplete phosphate and the positive surface to concentrate phosphate anions. Reversing the effects, Calvert and Mann [13] demonstrated that the relatively low charge density of phosphate anions made them compete effectively with chloride adsorption. On the Ca-implanted titanium surface, due to the dissociation of hydroxyl radicals, the surfaces are positively charged as measured by Hanawa [14]. Hence, it is very difficult to heterogeneously nucleate HA on the Ca-implanted titanium surface. Adsorption of solution-formed particles is proposed here as an alternative mechanism to heterogeneous nucleation.

The existence of Ca–P nanoparticles in the SBF solution has been shown by several researchers [25,17]. Tarasevich et al. [25] investigated the existence of nanoparticles in the SBF solution by the decreased concentrations of calcium and phosphate after passing them using ultrafine filters. Calcium depletion even occurred in solutions that did not contain the nucleation substrates. It is believed that the nanoparticles form in the solution formation process as it has been reported that conversion of a concentrated base to calcium- and phosphate-containing solution tends to increase the nanoparticle concentrations [25]. Onuma and Ito [17] further measured the size of the nanoparticles in the as-prepared SBF solution by intensity-enhanced dynamic light scattering technique to be 0.7–1.0 nm. Theoretically, clusters with a size smaller than that of the critical nucleus can exist stably in solutions when size-dependent surface tension is taken into account according to the theory of homogeneous nucleation. Therefore, the formation of Ca–P clusters does not necessarily mean the commencement of precipitation of amorphous Ca–P [17]. It is well known that SBF is supersaturated with HA and OCP. In other words, this kind of solution is in a metastable condition. Nucleation may take place if changes occur in the solution. On the Ca-implanted titanium surface, due to the rapid dissociation of the hydroxyl radicals and calcium ions, supersaturation of the solution ensues thereby destroying the equilibrium. The concentration of the nanoparticles increases and the clusters grow by aggregation. The aggregated clusters are negatively charged [26] and attracted by electrostatic forces to deposit on the positively charged Ca-implanted titanium surface. After adsorption, further growth of the crystallites on the surface is indicated by the increasing crystallite size over time.

In order to exclude the natural deposition of the solution-formed particles onto the titanium surface, untreated titanium discs were incubated in a $2 \times$ SBF solution (the concentrations of $Ca^{2+}$ and $HPO_4^{2-}$ ions are two times higher than those in conventional SBF with the other ion concentrations unchanged) for 14 days. No Ca–P can be found on the surfaces demonstrating that Ca–P minerals cannot deposit on the titanium surface without the help of the electrostatic interaction in spite of higher $Ca^{2+}$ and $HPO_4^{2-}$ ion concentration in the solution. Ca–P precipitation on downwards placed Ca-implanted titanium surfaces proves the importance of the electrostatic interaction in the nucleation process and excludes the possibility of gravitational deposition of the Ca–P clusters.

The initial nanoparticle adsorption results in deposition amounts that are insignificant compared to those of the growth region, and yet the adsorption has profound effects on changing the interfacial chemistry. These changes may significantly affect the nucleation and growth process. Two cluster growth mechanisms have been postulated. Tarasevich et al. [25] believe that the growth occurs by ion-by-ion incorporation. The possibility of Ca–P growth by aggregation of the small Ca–P clusters has also been suggested [17,27]. Aggregation of polynuclear clusters or oligomers has also been found in oxyhydroxides such FeOOH and AlOOH. The deposited film after incubation in SBF for 7 days is analyzed by XRD and the results show that it is mainly composed of OCP with a typical (100) peak at about 4.7°, although we cannot accurately assign the peaks at about 26° and 32° because of the similar patterns between HA and OCP from 26° to 32°.

Our theoretical calculations also confirm that the first precipitated phase is OCP. In the classical nucleation model, the tendency for a crystal to form depends upon two thermodynamic factors. The first is the driving force for crystallization expressed either as the relative supersaturation or the Gibbs free energy of transfer from a supersaturated to an assumed saturated solution at the interface. The second is the activation energy barrier to diffusion from the bulk solution to the substrate. A more direct expression is the nucleation rate. The free energy changes in the SBF solution shows that the thermodynamic driving force for HA nucleation is much larger than that of OCP ($\Delta G_{\mathrm{HA}} = -7.75\ \mathrm{kJ\ mol^{-1}}$ and $\Delta G_{\mathrm{OCP}} = -2.97\ \mathrm{kJ\ mol^{-1}}$). A larger driving force does not always imply a higher nucleation rate. Owing to the much lower probability of the appropriate ion units needed to compose HA nucleus in the solution than OCP, the nucleation rate of OCP is higher than that of HA by 10 orders of magnitude in SBF. Such a low probability for HA makes it nearly impossible to form a critical nucleation density in the solution.

Ostwald's rule of stages based on the experimental results illustrates that the least thermodynamically stable Ca–P phase nucleates and grows first on the surface, followed by nucleation and growth of more thermodynamically stable phases [28]. The ease of nucleation and growth of Ca–P phases follows the following trend: DCPD > OCP > TCP > HA [29]. Nelson et al. [30] have reported that the nucleation of OCP is energetically favored because the surface energy of HA is higher than that of OCP. The existence of a large amount of $CO_3^{2-}$ in the Ca-implanted titanium surface also affects the apatite formation [31].

With longer incubation duration, larger sized globular particles appear on the top of the film. In the XRD spectrum, the peaks at about 4.7° nearly disappear and the intensity of the peaks between 26° and 32° increases. It means that the phase of the Ca–P that precipitates at the later stage is HA. It can be explained by the altered interfacial chemistry resulting from the adsorption of OCP and decreased supersaturation in the SBF solution after the precipitation of OCP in the first stage. A more thermodynamically stable phase precipitates at the later stage. It should be noted that the transformation of OCP to HA after long time incubation in SBF solution cannot be excluded as Iijima et al. [32] have detected the transformation of OCP to HA by XRD and SEM.

## 5. Conclusion

The process and mechanism of calcium phosphate nucleation and growth on Ca-implanted titanium surfaces are studied. XRD results show that OCP is precipitated on the Ca-implanted titanium surfaces after 7 days incubation in SBF. The typical OCP peaks at 4.7° and 9.4°, 9.7° disappear after 14 days incubation in SBF and only HA peaks is used to explain the formation process of Ca–P phase on the Ca-implanted titanium surfaces as an alternative mechanism of heterogeneous nucleation. Our theoretical calculations show that HA is thermodynamically more stable than OCP, but the nucleation rate of OCP is much higher than HA in SBF solution.

## Acknowledgments

This work was supported by National Basic Research Fund under grant 2005CB623901, Shanghai Science and Technology R&D Fund under grant 03JC14074, Innovation Fund of SICCAS under grant SCX200410 and a Foundation for the Author of National Excellent Doctoral Dissertation of P.R. China (FANEDD), Hong Kong Research Grants Council (RGC) Central Allocation Group Research Project CityU 1/04C.

## References

[1] X.Y. Liu, P.K. Chu, C.X. Ding, Mater. Sci. Eng. Rep. 47 (2004) 49.
[2] T. Hanawa, H. Ukai, K. Murakami, K. Asaoka, Mater. Trans. JIM 36 (1995) 438.
[3] M.T. Pham, W. Matz, H. Reuther, E. Richter, G. Steiner, S. Oswald, Surf. Coat. Technol. 128–129 (2000) 313.
[4] N.N. Saima, H.J. Frances, O. Irwin, Biomaterials 26 (2005) 4717.
[5] T. Hanawa, Y. Kamiura, S. Yamamoto, T. Kohgo, A. Amemiya, H. Ukai, K. Murakami, K. Asaoka, J. Biomed. Mater. Res. 36 (1997) 131.
[6] T. Jinno, S.K. Kirk, S. Morita, V.M. Goldberg, J. Arthroplasty 19 (2004) 102.
[7] X.Y. Liu, R.W.Y. Poon, S.C.H. Kwok, P.K. Chu, C.X. Ding, Surf. Coat. Technol. 191 (2005) 43.
[8] K. Motojima, K. Furuya, S. Morita, S. Hasegawa, T. Hanawa, O. Okuno, K. Murakami, J. Jpn. Orthop. Assoc. 66 (1992) 1117.
[9] T. Hanawa, H. Ukai, K. Murakami, J. Electron Spectrosc. 63 (1993) 347.
[10] T. Hanawa, K. Asami, K. Asaoka, Microdissolution of calcium ions from Ca-implanted titanium, Corros. Sci. 38 (1996) 1579.
[11] K. Yamashita, N. Oiawa, T. Umegaki, Chem. Mater. 8 (1996) 2697.
[12] X.Y. Liu, C.X. Ding, P.K. Chu, Biomaterials 25 (2004) 1755.
[13] P. Calvert, S. Mann, Nature 386 (1997) 127.
[14] H. Hanawa, Mater. Sci. Eng. A—Struct. 267 (1999) 260.
[15] R.W.Y. Poon, K.W.K. Yeung, X.Y. Liu, P.K. Chu, C.Y. Chung, W.W. Lu, K.M.C. Cheung, D. Chan, Biomaterials 26 (2005) 2265.
[16] A.E. Nielsen, J. Cryst. Growth 67 (1984) 289.
[17] K. Onuma, A. Ito, Chem. Mater. 10 (1998) 3346.
[18] A. Ito, K. Maekawa, S. Tsutsumi, F. Ikazaki, T. Tateishi, J. Biomed. Mater. Res. 36 (1997) 522.
[19] H. McDowell, T.M. Gregory, W.E. Brown, J. Res. NBS—A Phys. Chem. 81A (1977) 273.

[20] J.C. Heughebaert, G.H. Nancollas, J. Chem. Eng. Data 30 (1985) 279.
[21] J.W. Mullin, Crystallization, third ed., Butterworth-Heinemann, Oxford, 1993, p. 172.
[22] R. Boistelle, I. Lopez-Valero, J. Cryst. Growth 102 (1990) 609.
[23] W. Wu, G.H. Nancollas, Adv. Coll. Interface Sci. 79 (1999) 229.
[24] K. Healey, P. Ducheyne, Biomaterials 13 (1992) 553.
[25] B.J. Tarasevich, C.C. Chusuei, D.L. Allara, J. Phys. Chem. B 107 (2003) 10367.
[26] P.X. Zhu, M. Ishikawa, W.S. Seo, A. Hozumi, Y. Yokogawa, K. Koumoto, J. Biomed. Mater. Res. 59 (2002) 294.
[27] K. Onuma, A. Oyane, K. Tsutsui, K. Tanaka, G. Treboux, N. Kanzaki, A. Ito, J. Phys. Chem. B 104 (2000) 10563.
[28] Ný vlt, J. Cryst. Res. Technol. 4 (1995) 443.
[29] L. Song, A.A. Campbell, X.S. Li, B.C. Bunker, Mater. Res. Soc. Symp. Proc. 414 (1996) 35.
[30] D.G.A. Nelson, J.C. Barry, C.P. Shields, R. Glena, J.D.B. Featherstone, J. Coll. Interface Sci. 130 (1989) 467.
[31] M. Iijima, H. Kamemizu, N. Wakamatsu, T. Goto, Y. Doi, Y. Moriwaki, J. Cryst. Growth 135 (1994) 229.
[32] M. Iijima, H. Kamemizu, N. Wakamatsu, T. Goto, Y. Doi, Y. Moriwaki, J. Cryst. Growth 181 (1997) 70.